MCNPX ANALYSIS OF THE MEDICAL ISOTOPE PRODUCTION IN THE KHARKOV ELECTRON DRIVEN SUBCRITICAL FACILITY

Alberto Talamo, Yousry Gohar, and Dmitry Naberezhnev

Argonne National Laboratory, 9700 South Cass Avenue, Argonne, IL 60439, USA. Email: alby@anl.gov

One of the main functions of the planned Kharkov electron driven subcritical facility will be the production of medical isotopes. This facility function was examined, with particular attention to the self-shielding of the irradiated samples, by Monte Carlo simulations. The facility consists of a subcritical assembly fueled with low enriched uranium, cooled by water, and surrounded by graphite reflector. The self-shielding effect reduces the reaction rates in the irradiated sample, the specific activity of the produced medical isotopes, and it changes the irradiation position that maximizes the reaction rates. The analyses used the detailed three dimensional MCNPX model of the facility to compare the specific activity of ^{60}Co, ^{66}Cu, and ^{166}Ho, with and without the self-shielding effect, for four different positions in the subcritical assembly.

I. INTRODUCTION

Medical isotopes are very important to the general public because of their use to diagnose and treat many diseases. In the United States, one of every three hospitalized patients undergoes a nuclear medicine procedure and about 180000 patients were treated by a radiation therapy in 1990 (Ref. 1). These numbers are significantly increasing since newer nuclear medical procedures are being developed. Nuclear medical procedures use short lived nuclides to minimize the biological dose to the patient; therefore, a continuous supply of medical isotopes is required. In this paper, the production of medical isotopes at the planned Kharkov electron driven facility[2-4] in Ukraine has been studied with the inclusion of the self-shielding effect. The facility consists of an electron driven subcritical assembly surrounded by graphite, cooled by water and fuelled with WWR-M2 low enriched uranium (LEU) fuel. The beam power is 100 kW and the electron energy is 200 MeV. Electrons interact with the natural uranium target generating high energy photons, by the Bremsstrahlung effect,[5] that have a continuous energy spectrum. The high energy photons interact with the uranium target and fuel assembly generating neutrons through photonuclear fissions[6] and (γ,xn) reactions.[7] Photonuclear reactions require a photon energy above 5 MeV and their cross sections rapidly drop above 25 MeV. The giant resonance of the photonuclear cross sections occurs at about 15 MeV.[8-9] The Kharkov subcritical assembly geometrical details are shown in figures 1 and 2 (Ref. 10). The cost of medical isotopes production using electron driven facilities is smaller than the

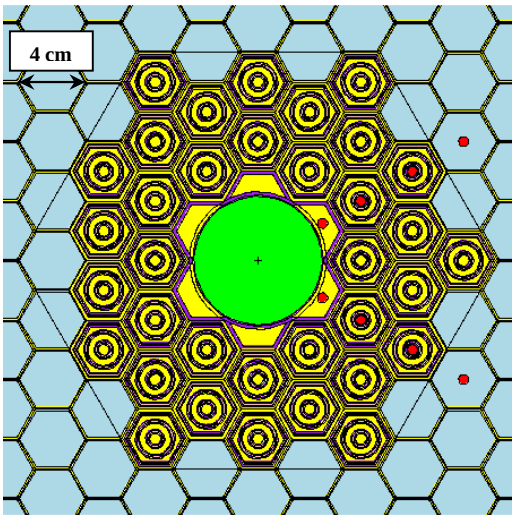

Fig. 1. Horizontal cross section of the subcritical assembly. Red=medical isotopes samples, light blue=graphite, yellow=water, green=natural uranium, purple=aluminum, pink=enriched uranium.

one using proton driven facilities because of the cheaper accelerator hardware cost and lower power consumption. Electrons are easier to accelerate, compared to protons, due to their much smaller mass; however, some medical isotopes require incident proton reactions.[11-12]

This paper focuses on the comparison of the specific activities of ^{60}Co, ^{66}Cu and ^{166}Ho, obtained with and without considering the self-

shielding effect, for four different irradiation locations in the subcritical assembly. The first location is close to the target, the second one is at the center of an inner fuel assembly next to the target, the third one is at the center of an outer fuel assembly next to the reflector, and the fourth one is at the center of the first graphite reflector block next to the subcritical assembly fuel, as illustrated in figure 1.

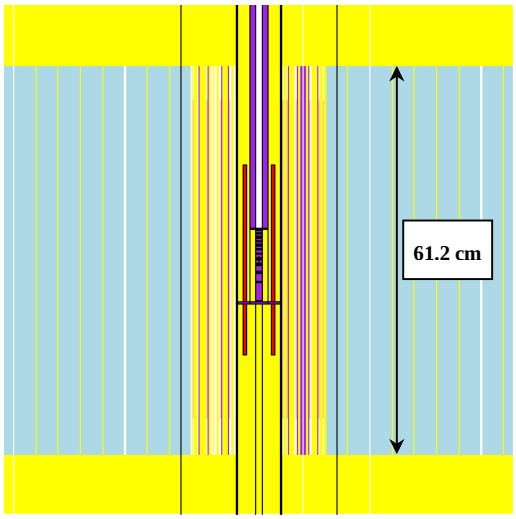

Fig. 2. Vertical cross section of the subcritical assembly. Red=medical isotopes samples, light blue=graphite, yellow=water, green=natural uranium, purple=aluminum, pink=enriched uranium, white=vacuum.

II. EVALUATION OF THE SPECIFIC ACTIVITY

In the analyses, natural materials have been used as parent nuclides of the medical isotopes. The initial atomic density of the parent nuclide N_p^0 is given by Eq. (1), where d_{nat} is the natural density of the parent material, A is the Avogadro's number, f is the natural abundance of the parent nuclide in the parent material and W the atomic weight of the parent material.

$$N_p^0 = \frac{d_{nat} \cdot A \cdot f}{W} \qquad 1)$$

The atomic density N of the daughter nuclides (medical isotopes) has been calculated by solving the system of Eq. (2a), whose solution is given by Eq. (2b), where λ is the decay constant of the daughter nuclide, N_p is the density of the parent nuclide, and $\sigma_p\Phi$ is the parent reaction rate per nuclide. The specific activity of the medical isotope is λN. The parent reaction rate per nuclide has been obtained by multiplying the reaction rate per nuclide and source particles obtained from the MCNPX calculations[13] by the number of source particles (electrons) per second. The MCNPX standard deviation of the calculated reaction rates per nuclide and source particle is lower than 0.3%. In all analyses, the daughter reaction rate per nuclide $\sigma\Phi$ has been neglected because of its low value relative to the decay constant (medical isotopes are short-life nuclides).

$$\begin{cases} \dfrac{dN}{dt} = -(\lambda + \sigma\Phi)N + \sigma_p N_p \Phi \\ \dfrac{dN_p}{dt} = -\sigma_p N_p \Phi \end{cases} \qquad 2a)$$

$$N(t) = \sigma_p \Phi N_p^0 \frac{e^{-\sigma_p \Phi t} - e^{-(\lambda+\sigma\Phi)t}}{\lambda + \sigma\Phi - \sigma_p\Phi} \qquad 2b)$$

In the MCNPX simulations without self-shielding, the irradiation locations have not been filled by the parent materials; on the contrary to the accurate calculations with the self-shielding effect. In the calculations without self-shielding, the irradiated samples consist of a cylindrical wire with 0.3 cm radius and 30 cm length. The length has been reduced down to 5 cm for the self-shielding analyses.

III. ANALYSIS WITHOUT SELF-SHIELDING

The analyses without self-shielding factor have been performed for more than 50 parent nuclides. After 15 irradiation days, the results show that ^{82}Br, ^{64}Cu, ^{165}Dy, ^{166}Ho, ^{192}Ir, ^{194}Ir, ^{186}Re, ^{188}Re and ^{153}Sm have a specific activity larger than 100 MBq/mg. ^{60}Co, ^{51}Cr, ^{159}Gd, ^{24}Na, ^{32}P (via (n,γ)), and ^{90}Y have a specific activity between 10 and 100 MBq/mg. ^{111}Ag, ^{125}I, ^{42}K, ^{99}Mo, ^{32}P (via (n,p)), ^{99m}Tc and ^{133}Xe (via (n,γ)) have a specific activity between 1 and 10 MBq/mg. ^{58}Co, ^{67}Cu, ^{59}Fe, ^{177m}Lu, ^{33}P, ^{103}Pd, ^{35}S, ^{47}Sc, ^{188}W and ^{133}Xe (via (n,2n) and (n,p)) have a specific activity lower than 1 MBq/mg. ^{58}Co, ^{60}Co, ^{51}Cr, ^{59}Fe, ^{125}I, ^{192}Ir, ^{177m}Lu, ^{33}P, ^{35}S, ^{47}Sc, and ^{188}W require an irradiation time longer than 100 days to reach the specific activity asymptotic level. Generally, the production rate is driven by the following rules:

- Isotopes generated through large thermal cross sections are better produced in the fourth location, in the graphite reflector. This irradiation location has the highest thermal neutron flux.

- Isotopes generated through resonances in the slowing down energy range are better produced in the first location, in the target water channel. This irradiation location has the highest epithermal neutron flux.
- Isotopes generated through threshold cross sections, e.g. (n,2n) and (n,p), are better produced in the second location, inside the fuel assembly next to the target. This irradiation location has the highest fast neutron flux.

IV. ANALYSIS WITH SELF-SHIELDING

The self-shielding effect can be analytically predicted for foils;[14-15] however, we utilized a more pragmatic approach using MCNPX. In this approach, the parent materials are modeled inside the irradiation location for calculating the reaction rates. This paper focuses on ^{59}Co, ^{63}Cu and ^{165}Ho parent isotopes because they have similar macroscopic cross sections; this feature facilitates the comparison of the obtained results. Figures 3 to 5 compare the specific activities of the corresponding medical isotopes without and with self-shielding. Few general observations emerge from these results:

- At the fourth irradiation location, the self-shielding effect increases as the macroscopic cross section value of the parent nuclide for producing the radioactive isotope at 10^{-5} eV increases. In the thermal energy range, the microscopic cross sections exhibit the 1/v linear dependence and a smaller slope increases the self-shielding.
- At the first and the fourth locations, large resonance cross sections increase the self-shielding effect. However, this effect is observed more in the first irradiation location due to its high neutron flux in the slowing down energy range.
- The irradiation of a natural material with multiple isotopes (copper) enhances the self-shielding effect due to the resonances overlapping (especially for the first location) or to the high value of the cross sections at the thermal energy (especially for the fourth location). The effect is amplified at the first irradiation location because of its high neutron flux in the slowing down energy range.

At 10^{-5} eV neutron energy, the (n,γ) macroscopic cross sections of ^{63}Cu, ^{165}Ho and

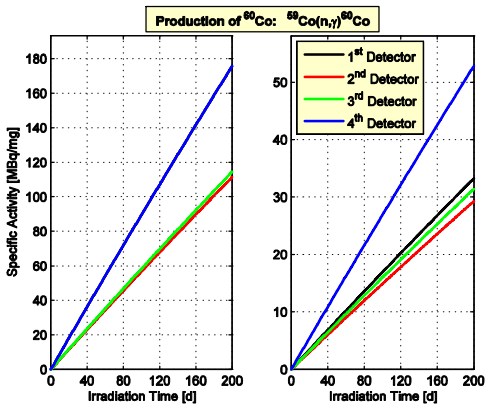

Fig. 3. ^{60}Co activity as a function of the irradiation time without and with self-shielding, left and right subplots, respectively; ^{60}Co represents 100% of the parent material.

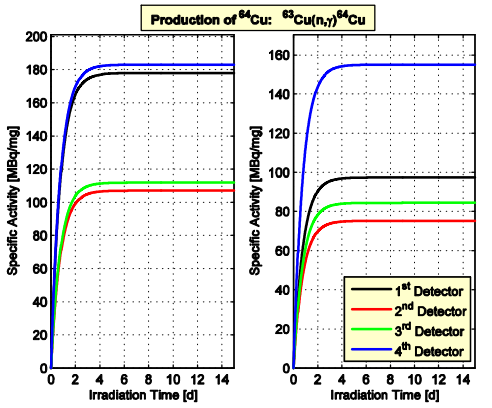

Fig. 4. ^{64}Cu activity as a function of the irradiation time without and with self-shielding, left and right subplots, respectively; ^{63}Cu and ^{65}Cu represent 69.17 and 30.83% of the parent material, respectively.

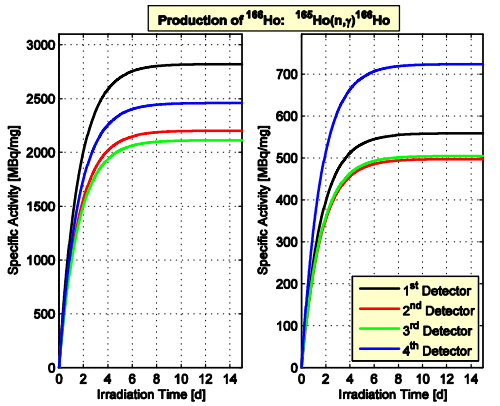

Fig. 5. ^{166}Ho activity as a function of the irradiation time without and with self-shielding, left and right subplots, respectively; ^{165}Ho represents 100% of the parent material.

^{59}Co are ~10, 100 and 200 cm^{-1}, respectively. These cross section values changes to ~1 cm^{-1} at neutron energies of 0.001, 0.1 and 0.1 eV, respectively. The calculated self-shielding factors for the specific activity of the daughter isotopes at the fourth irradiation location are 1.16, 3.8, and 3.3, respectively. The comparison between ^{165}Ho and ^{59}Co is simplified since their abundances are 100% in the natural material. At the fourth irradiation location, the self-shielding factor for ^{60}Co is smaller than the corresponding value for ^{166}Ho although the thermal (n,γ) macroscopic cross section at 10^{-5} eV is about double. The higher (n,γ) macroscopic cross section of ^{165}Ho, for neutron energy above 2 eV, than the corresponding macroscopic cross section of ^{59}Co, explains the previous result. Because of the high resonances of the microscopic cross section in the slowing down energy range, the fourth irradiation location is the best for producing ^{166}Ho isotope, which is a different result relative to the simulations ignoring the self-shielding. For the production of ^{64}Cu, the resonances overlapping of ^{63}Cu and ^{65}Cu reduces the production of ^{64}Cu in the first location more than in the fourth one.

V. CONCLUSIONS

These studies have proven the importance of the self-shielding effect for medical isotopes production when the facility works on a thermal neutron spectrum. The self-shielding effect reduces the specific activity of the medical isotopes and it also changes the irradiation location that maximizes the production rate. These two effects amplify when the parent nuclides have a large microscopic cross section in the thermal energy range or when they exhibit large resonances. The study quantified ^{60}Co, ^{64}Cu and ^{166}Ho production in the Kharkov electron driven subcritical facility.

ACKNOWLEDGMENTS

This project is supported by the U.S. Department of Energy, Office of Global Nuclear Material Threat Reduction (NA213), National Nuclear Security Administration and the Science and Technology Center in Ukraine (STCU).

REFERENCES

[1] S.J. ADELSTEIN, T.F. BUDINGER, R.E. COLEMAN, D. DANFORD, W.C. ECKELMAN, J.A. NOLEN, L.L. RIEDINGER, T.J. RUTH, L.S. SCHROEDER, M.J. WELCH, S.W. YATES, *Isotopes for Medicine and Life Science*, National Academy Press, ISBN 0-309-05190-8, (1995).

[2] Y. GOHAR, J. BAILEY, H. BELCH, D. NABEREZHNEV, P. STRONS and I. BOLSHINSKY, "Accelerator-Driven Subcritical Assembly: Concept Development and Analyses," *RERTR-2004 International Meeting on Reduced Enrichment for Research and Test Reactors*, (2004).

[3] Y. GOHAR, I. BOLSHINSKY, D. NABEREZHNEV, J. DUO, H. BELCH and J. BAILEY, "Accelerator-Driven Subcritical Facility: Conceptual Design Development," *Nuclear Instruments & Methods in Physics Research A* **562**, pp. 870-874, (2006).

[4] D. NABEREZHNEV, Y. GOHAR, J. BAILEY and H. BELCH, "Physics Analyses of an Accelerator-Driven Subcritical Assembly," *Nuclear Instruments & Methods in Physics Research A* **562**, pp. 841-844, (2006).

[5] Y.M. ADO, K.A. BELOVINTSEV and S.N. STOLYAROV, "The Bremsstrahlung Spectrum of Electrons with an Energy of 260 MeV," *Atomic Energy* **12/3**, pp. 193-197, (1962).

[6] C.D.BOWMAN,G.F. AUCHAMPAUGH and S.C. FULTZ, "Photodisintegration of ^{235}U," *Physical Review* **133/3b**, pp. 676-683, (1964).

[7] M.B. CHADWICK, P.G. YOUNG, R.E. MACFARLANE, M.C. WHITE, and R.C. LITTLE, "Photonuclear Physics in Radiation Transport—I: Cross Sections and Spectra," *Nuclear Science and Engineering* **144**, pp. 157-173, (2003).

[8] M.L. GIACRI-MAUBORGNE, D. RIDIKAS, M.B. CHADWICK, P.G. YOUNG, and W.B. WILSON, "Photonuclear Physics in Radiation Transport—III: Actinide Cross Sections and Spectra," *Nuclear Science and Engineering* **153**, pp. 33-40, (2006).

[9] D. RIDIKAS, M.L. GIACRI, M.B. CHADWICK, J. C. DAVID, D. DORE´, X. LEDOUX, A. Van LAUWE AND W.B. WILSON, "Status of the photonuclear activation file: Reaction cross-sections, fission fragments and delayed neutrons," *Nuclear Instruments & Methods in Physics Research A* **562**, pp. 710-713, (2006).

[10] A. Talamo and Y. Gohar, *Radioactive Isotope Production for Medical Applications Using Kharkov Electron*

Driven Subcritical Assembly Facility, Argonne National Laboratory, ANL-07/18, (2007).

[11] K. A. Van RIPER, S.G. MASHNIK and W.B. WILSON, "A computer study of radionuclide production in high power accelerators for medical and industrial applications," *Nuclear Instruments & Methods in Physics Research A* **463**, pp. 576-585, (2001).

[12] S. MIRZADEH, C.W. ALEXANDER, T. Mc MANAMY and F.F. KNAPP, *Projected Medical Radioisotope Production Capabilities of the Advanced Neutron Source (ANS)*, Oak Ridge National Laboratory, ORNL/TM-10210-S, (1994).

[13] J.S. HENDRICKS et al., *MCNPX, VERSION 2.6.B*, Los Alamos National Laboratory, LA-UR-06-3248, (2006).

[14] M. NEVES, A. KLING and R.M. LAMBRECHT, "Radionuclide Production for Therapeutic Radiopharmaceuticals," *Applied Radiation and Isotopes* **57**, pp. 657-664, (2002).

[15] M. Do CARMO LOPES and J. MOLINA AVILA, "Multiple Scattering Resonance Self Shielding Factors in Foils," *Nuclear Instruments & Methods in Physics Research A* **280**, pp. 304-309, (1989).